Jordan Lluch, C.; Morillas, S.; Sanabria Codesal, E. (2012). Colour image smoothing through a soft-switching mechanism using a graph model. IET Image Processing. 6(9):1293-1298. doi:10.1049/IET-IPR.2011.0164.

Colour image smoothing through a soft-switching mechanism using a graph model

C. Jordán[⋆], S. Morillas[◇*] and E. Sanabria-Codesal[◇*]

([⋆]) Instituto Universitario de Matemática Multidisciplinar (IMM)

([◇]) Instituto Universitario de Matemática Pura y Aplicada (IUMPA)

Universitat Politècnica de València, Camino de Vera s/n, 46022 Valencia, Spain

Email addresses: cjordan@mat.upv.es, smorillas@mat.upv.es, esanabri@mat.upv.es

July 24, 2012

Abstract

In this paper we propose a soft-switching filter to improve the performance of recent colour image smoothing filters when processing homogeneous image regions. We use a recent filter mixed with the classical arithmetic mean filter (AMF). The recent method is used to process image pixels close to edges, texture and details and the AMF is only used to process homogeneous regions. To this end, we propose a method based on graph theory to distinguish image details and homogeneous regions and to perform a soft-switching between the two filters. Experimental results show that the proposed method provides improved results which supports the

[*]The authors acknowledge the support of Spanish Ministry of Science and Innovation under Grant MTM2009-12872-C02-01, Spanish Ministry of Science and Technology under grant MTM2010-18539 and DGCYT under grant MTM2009-08933

appropriateness of the graph theory-based method and suggests that the same structure can be used to improve the performance of other nonlinear colour image smoothing methods.

Keyword: Colour image smoothing, Graph theory, Kruskal algorithm

1 Introduction

Colour image denoising is a topic which has been extensively studied in the fields of computer vision and digital image processing. The denoising (or filtering) step is essential for almost every computer vision system because noise can significantly affect the visual quality of the images as well as the performance of most automatic image processing tasks. Among the different sources of noise in digital imaging, probably the most common one is the so-called thermal noise, which is mainly due to CCD sensor malfunction and specially intense with inappropriate illumination conditions. This kind of noise is modeled as additive white Gaussian noise [1].

Many methods for reducing Gaussian noise from colour images have been proposed in the literature [1, 2], with the aim of smoothing image noise while keeping intact desired image features such as edges, texture and fine details. The earliest approaches for Gaussian noise smoothing were based on a linear approach. These methods, such as the *Arithmetic Mean Filter* (AMF) [1], are able to suppress noise, because they take advantage of its zero-mean property, but they blur edges and texture significantly. This fact motivated the development of many nonlinear methods that try to overcome this drawback. Within the nonlinear methods, we can find families of filters based on different approaches, such as weighted averaging [3, 4, 5], peer group averaging [6], fuzzy logic or soft switching [7, 8, 9, 10], regularization filters [11], and wavelet filtering [12, 13].

Recent nonlinear methods exhibit an improved performance with respect to the linear approaches, above all, from the edge and detail preservation point of view, since they try to detect and preserve these features. However, as the noise in the image is higher, many times image noise in homogeneous regions is confused with an image structure that should be preserved and so it is not properly reduced. In this paper we propose a method to improve performance by overcoming this drawback. We propose a robust method based on graph theory to classify image pixels into two classes: homogeneous regions and edge-detail regions. Then, we use the AMF to process image homogeneous regions since it is the filtering structure providing the maximum smoothing capability. To process the rest of the image, we use a recent nonlinear method called *Fuzzy Noise Reduction Method* (FNRM) [7]. The switching between AMF and FNRM is performed in a soft fashion so that when the class of the image pixel is not clearly determined the results of both methods are combined. The proposed filter follows the idea presented in [8] but including a new graph-based classification criteria that allows to achieve high level performance. Also, notice that although we have used the FNRM, any other nonlinear method can be used within the same structure and similar improvements are expected.

In the following section we review the basics on graph theory and Section 3 describes the graph-based classification method. Section 4 describes the proposed filtering structure. Experimental results are shown in Section 5 and some conclusions are drawn in Section 6.

2 Fundamentals of graph theory

A graph G is defined as a finite nonempty set $V(G)$ of objects called vertices and a set $E(G)$ of unordered pairs of distinct vertices of G called edges. A graph H

is called a subgraph of G if $V(H) \subseteq V(G)$ and $E(H) \subseteq E(G)$. If $V(H) = V(G)$ then H is also called a spanning subgraph of G.

A walk W from a vertex v_0 to a vertex v_l in a graph is an alternating sequence of vertices and edges, say $v_0, e_1, v_1, e_2, \ldots, e_l, v_l$ where $e_i = (v_{i-1}, v_i)$, $0 < i \leq l$. If a walk $W = v_0, e_1, v_1, e_2, \ldots, e_l, v_l$ is such that $l \geq 3$, $v_0 = v_l$ and the vertices v_i, $0 < i < l$, are distinct from each other and v_0, then W is said to be a cycle. A graph is connected if for every pair $\{v_i, v_j\}$ of distinct vertices there is a walk from v_i to v_j. A connected graph G without any cycles is a tree. A graph is called complete if every pair of vertices is joined by an edge.

A weighted graph is a graph in which each edge e is assigned a real number $w(e)$. The weight $w(H)$ of a subgraph H of a weighted graph is the sum of the weights of the edges of H, that is $w(H) = \sum_{e \in E(H)} w(e)$.

A spanning tree T of G having minimum (maximum) weight is called a minimum (maximum) spanning tree. The Kruskal's algorithm [14] allows to determine a minimum (maximum) spanning tree of a connected graph G.

3 Detection of homogeneous regions using graphs

In this work we will use digital colour images represented in the Red-Green-Blue (RGB) colour space using 24 bits per pixel. This implies that each image pixel is associated with a tern of values that represents the coordinates of the colour of that pixel. Let us denote a digital image by $\mathbf{F}$ and each image pixel by $\mathbf{F_i} = (F_i^R, F_i^G, F_i^B)$, where $F_i^R, F_i^G, F_i^B \in [0, 255]$.

Our method processes the digital image $\mathbf{F}$ by means of a sliding window approach. Each image pixel $\mathbf{F}_i$ is processed independently using the pixels in a $n \times n$ processing window Ω centered on $\mathbf{F}_i$. For convenience, we denote the $N = n^2$ colour pixels in Ω by $\{\mathbf{F}_1, \ldots, \mathbf{F}_N\}$.

Our method first classifies image pixels into homogeneous regions and edge-detail regions. For this we will use a method based on graphs, in particular, on maximum and minimum spanning trees. Associated to each sliding window Ω we define a weighted complete graph which has as vertices $V(G)$ the set of colour image pixels in Ω, that is, $V(G) = \{\mathbf{F}_1, \ldots, \mathbf{F}_N\}$. The weight of an edge $w(e_k) = w(\mathbf{F}_i, \mathbf{F}_j) = \|\mathbf{F}_i - \mathbf{F}_j\|$, where we use the Euclidean norm of the difference between $\mathbf{F}_i$ and $\mathbf{F}_j$ to represent the dissimilarity between these two colours.

Then, we use the Kruskal algorithm [14] to determine the minimum and maximum spanning trees of G, which we denote by K_m and K_M, respectively. Considering the weights of K_m and K_M we define the following coefficients, which will be used to perform the desired classification:

$$C_1 = \frac{\log w(K_m)}{w(K_M)}, C_2 = \frac{w(K_m) - w(K_M)^2}{W}, \text{ where } W = w(G).$$

The reasoning behind these coefficients is that their values will be very different in homogeneous and edge-detail regions of the image even in the presence of noise. Indeed, $w(K_M)$ and $w(K_m)$ will be quite alike in homogeneous regions since all edges will have similar weights and so will be the global weight of the minimum and maximum spanning trees. In the presence of noise, some edge weights may be larger and others may be smaller, but since all pixels (vertices) are involved in the computation of the spanning trees, no large differences are expected between $w(K_M)$ and $w(K_m)$, which implies the method is robust to the presence of noise. On the other hand, $w(K_M)$ and $w(K_m)$ will be pretty different in edge-detail regions. This happens because in these regions there exist some edges with large weights and others with low weights. Most of the former will be included in K_M whereas the majority of the latter will be in K_m, which implies that $w(K_M)$ and $w(K_m)$ will be quite different, regardless the presence of noise. The expressions

to determine C_1 and C_2 exploit these facts, making use of logarithms and squares to enhance the difference between $w(K_M)$ and $w(K_m)$ when appropriate. For C_1 and C_2 larger values are associated to homogeneous regions whereas lower values correspond to edge-detail regions, as we can observe in Fig. 1 where we denote with $N(Ci),\ \ i = 1, 2$ the normalized values of the corresponding coefficients and with $N(w(K_M) - w(K_m))$ the normalized one for the difference between $w(K_M)$ and $w(K_m)$.

Figure 2 illustrates the performance of C_1 and C_2 with respect to the classification of the homogeneous and edge-detail regions of the image, where the bright and dark zones correspond to homogeneous and edge-detail regions, respectively. Notice that our purpose is not to devise a pure edge detection method since to properly detect edges more criteria concerning connection and single edge detection should be considered. So, the only advantage of our approach in front of edge detection methods is related to its robustness against noise, which is indeed our objective as explained above.

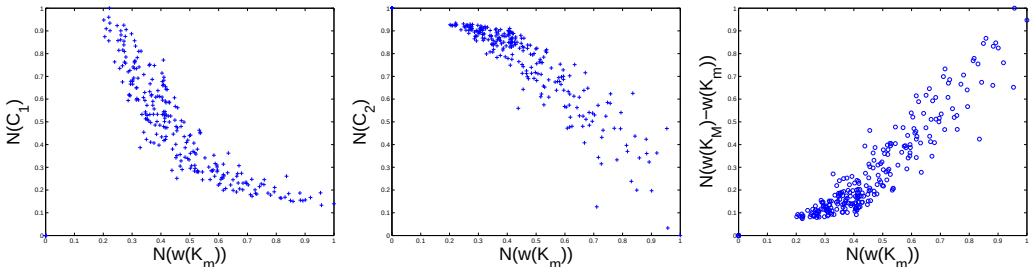

(a) (b) (c)

Figure 1: Relationship between $N(w(K_m))$ and (a) $N(C_1)$, (b) $N(C_2)$ and (c) $N(w(K_M) - w(K_m))$ at each pixel in the Pills image with gaussian noise $s = 10$.

4 Soft-switching filtering structure

The proposed denoising method called *Soft-Switching Graph Denoising Method* (SSGD) uses the AMF to process homogeneous regions of the image, whereas

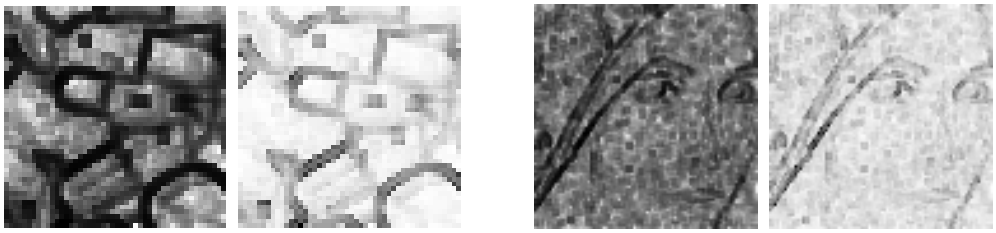

(a) (b) (c) (d)

Figure 2: Classification in edge-detail and homogeneous regions for the Pills image with gaussian noise $s = 10$ using (a) C_1 and (b) C_2, and for the Lenna image with gaussian noise $s = 30$ using (c) C_1 and (d) C_2.

the FNRM is employed to filter pixels in edge-detail regions. The switching between these two methods is done in a soft fashion. So, the output of the proposed method, $SSGD_{out}$, will be obtained through a weighted combination of the outputs of the two filters AMF_{out} and $FNRM_{out}$ as

$$SSGD_{out} = \alpha AMF_{out} + (1 - \alpha) FNRM_{out},$$

for each image pixel. Notice that when $\alpha = 1$ SSGD behaves as the AMF, and when $\alpha = 0$ SSGD equals FNRM. Thus, the value of α should depend on the nature of the pixel under processing. That is, if the pixel belongs to an homogeneous region of the image α should be large (closer to 1), otherwise, α should be lower (closer to 0).

To decide whether the particular pixel belongs to one type of region or the other we use the coefficients C_1 and C_2. It should be pointed out that the values of these coefficients can vary significantly for different images depending on their features such as image colour range, sharpness of edges, quantity of texture in the image, etc. So, after computing the value of the coefficient for all image pixels, we normalize the obtained values to the interval $[0, 1]$ in a linear way, which will ease the processing of different images.

If using C_1, we know that "if C_1 is large, then the pixel belongs to an ho-

mogeneous region". Since "C_1 is large" is a vague statement, it can be modeled using fuzzy theory [15]. So, we use a membership function that provides a value in $[0, 1]$ that represents the certainty degree of the vague statement. In this case, we have selected a S-type membership function μ defined as in [15]:

$$\mu(x, a, b) = \begin{cases} 0 & \text{if } x < a \\ 2\left(\frac{x-a}{b-a}\right)^2 & \text{if } a \leq x \leq \frac{a+b}{2} \\ 1 - 2\left(\frac{x-b}{b-a}\right)^2 & \text{if } \frac{a+b}{2} < x \leq b \\ 1 & \text{if } x > b \end{cases}, \tag{1}$$

where a, b are two function parameters. Thus, we can directly assign $\alpha = \mu(C_1, a, b)$ so that we obtain the weight that makes our denoising method behave as desired. An analogous process can be followed for the coefficient C_2.

5 Experimental results and comparisons

In the experimental section we have used the test images (Fig. 3) Lenna, Pepper, Parrot, Pills, Aerial and Baboon. These images have been corrupted with noise using the classical white additive Gaussian model [1]. Each colour image channel has been contaminated independently varying the standard deviation s which represents the noise intensity. To assess the performance of the filtering process, we use the *Peak Signal to Noise Ratio* (PSNR) as defined in [1, 2]. Notice that other types of noise such as impulsive noise or alpha-stable noise also affect colour images. However, we focus on the study of the additive white Gaussian noise since FNRM, AMF and our edge-detail detection method are devised for this type of noise and we believe that the method will not be appropriate for other types of noise in general, although it might perform well in particular noise ranges.

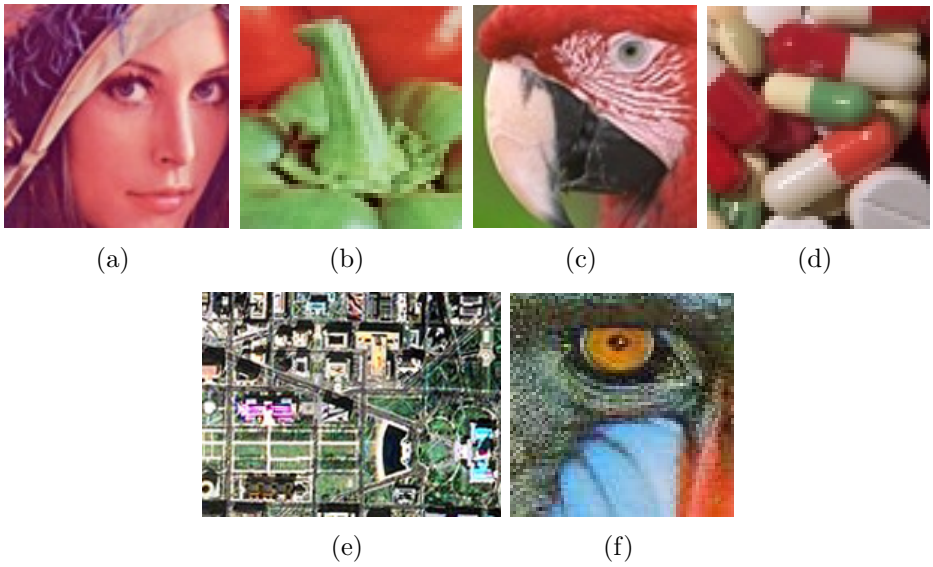

Figure 3: Test images : (a) Lenna, (b) Pepper, (c) Parrot, (d) Pills, (e) Aerial, and (f) Baboon.

First, we need to find appropriate settings for the parameters a, b in Eq. (1). To this end, we have experimentally analyzed the filter performance in terms of PSNR as a function of these parameters. The images Lenna, Parrot, Pepper and Pills (Figure 3 (a), (b), (c) and (d)) have been contaminated with noise varying s in $\{10, 20, 30\}$ and the performance in terms of PSNR has been calculated for different values of $a, b \in [0, 1]$. We have observed that optimal parameter setting depends on both noise density and the image to be processed. However, we have seen that the settings in Table 1 are able to provide sub-optimal performance. In fact, the settings of the a and b parameters are not critical for the filter performance. We have observed that varying the value of a and b in the intervals in Table 1 leads to PSNR differences lower than 0.5 units, which implies that any value in these intervals can be safely used. Notice that the standard deviation of the corrupting Gaussian noise s can be estimated using the method in [16], so the information in Table 1 can be used to set the parameters for processing any input image.

Table 1: Intervals of parameter sub-optimal performance and suggested parameter setting for different noise densities obtained through experimental evaluation

Coefficient	C_1			C_2		
	$s = 10$	$s = 20$	$s = 30$	$s = 10$	$s = 20$	$s = 30$
sub-optimal range for a	$[0.1, 0.3]$	$[0, 0.2]$	$[0, 0.3]$	$[0.8, 0.9]$	$[0.7, 0.8]$	$[0.55, 0.65]$
robust setting for a	0.10	0.10	0.10	0.90	0.75	0.55
sub-optimal range for b	$[0.65, 0.9]$	$[0.5, 0.9]$	$[0.5, 0.7]$	$[0.95, 1]$	$[0.95, 1]$	$[0.9, 1]$
robust setting for b	0.85	0.75	0.60	1.00	1.00	1.00

Now, using the parameter setting in Table 1, the test images in Figure 3 contaminated with different densities of noise have been processed using the AMF, FNRM and the proposed SSGD method with the coefficients C_1 and C_2. As above, the quality of the filtered images has been evaluated using the PSNR quality measure. These numerical results are given in Tables 2, 3.

Table 2: Performance comparison in terms of PSNR using the images contaminated with different standard deviation of Gaussian noise

Filter	PillsD			PeppersD			ParrotsD2			LennaD		
	10	20	30	10	20	30	10	20	30	10	20	30
None	28.40	22.59	19.21	28.55	22.48	19.16	19.16	22.44	19.16	19.17	22.54	19.17
AMF	25.90	25.21	24.14	26.50	25.62	24.61	23.36	22.91	22.33	27.69	26.61	25.28
FNRM	32.28	28.14	25.13	32.14	27.84	25.16	30.84	27.36	24.66	32.53	28.14	25.20
SSGD C_1F	32.40	**28.90**	26.13	32.44	**28.65**	26.36	30.91	**27.94**	**25.45**	32.82	29.04	26.50
SSGD C_2F	**32.48**	28.89	**26.17**	**32.47**	28.62	**26.39**	**30.94**	27.92	25.26	**32.86**	**29.12**	**26.55**

Table 3: Performance comparison in terms of PSNR using the images contaminated with different standard deviation of Gaussian noise

Filter	Aerial			Baboon		
	10	20	30	10	20	30
None	28.42	22.55	19.23	28.34	22.17	19.47
AMF	18.90	18.68	18.37	23.26	22.86	22.70
FNRM	**27.39**	25.37	23.37	30.12	27.08	24.65
SSGD C_1F	**27.39**	**25.38**	23.38	30.13	27.20	**25.00**
SSGD C_2F	**27.39**	**25.38**	**23.40**	**30.14**	**27.21**	24.99

We can see that the quality of the AMF is clearly below the rest of the methods. On the other hand, we can see that the SSGD method is in general able to provide improved performance with respect to the FNRM. The numerical results indicate that the improvements obtained are higher for higher noise and for images with larger homogeneous regions than for high frequency images (Aerial and Baboon). Some of these filtered images are shown in Figs. 4-6 for

visual inspection. Also, we tested the performance of our proposal over an image contaminated with real noise (see Fig. 7).

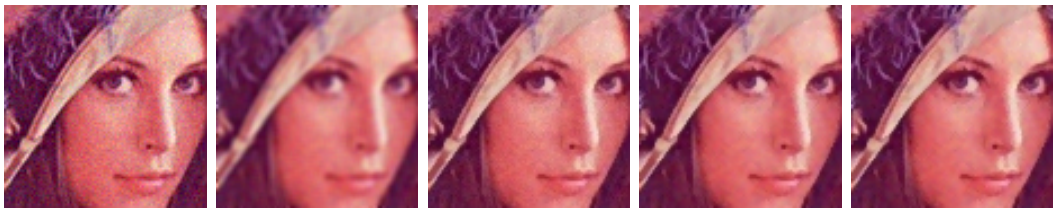

(a) (b) (c) (d) (e)

Figure 4: Experimental results: (a) Lenna image contaminated with noise $s = 10$ and outputs from (b) AMF, (c) FNRM, (d) SSGD C_1 with $a = 0.1, b = 0.85$ and (e) SSGD C_2 with $a = 0.9, b = 1$.

(a) (b) (c) (d) (e)

Figure 5: Experimental results: (a) Pills image contaminated with noise $s = 20$ and outputs from (b) AMF, (c) FNRM, (d) SSGD C_1 with $a = 0.1, b = 0.75$ and (e) SSGD C_2 with $a = 0.75, b = 1$.

In Figures 4-6 we can see that SSGD is able to smooth the noise in the homogeneous regions of the image better than FNRM, specially as the noise is higher, while keeping the same quality in edge-detail regions, which explains the PSNR improvement. This also confirms the good classification performed by the graph theory based method. These points are supported by the results over the real noisy image in Figure 7, where we can see that our filter produces the most visually pleasing image.

Finally, it is interesting to point out that, as this filtering structure has been used to improve the performance of the FNRM, it can be also used to improve the performance of other colour image smoothing methods.

(a) (b) (c) (d) (e)

Figure 6: Experimental results: (a) Parrots image contaminated with noise $s = 30$ and outputs from (b) AMF, (c) FNRM, (d) SSGD C_1 with $a = 0.1, b = 0.6$ and (e) SSGD C_2 with $a = 0.55, b = 1$.

6 Conclusions

In this paper, we deal with the problem of smoothing highly contaminated images where the performance of nonlinear methods can be improved, specially in homogeneous image regions. We propose to use a method based on graph theory to detect pixels in homogeneous regions, which are processed using the Arithmetic Mean Filter (AMF) to obtain the higher smoothing capability. The rest of the image pixels are processed using a recent nonlinear method and the switching between these two filters is implemented in a soft fashion. Experimental results show that the proposed approach outperforms the recent method used. Notice, that the same filter structure can be used with any other nonlinear method and similar improvements are expected.

(a) (b) (c)

(d) (e)

Figure 7: Experimental results: (a) An image contaminated with real noise acquired using a domestic camera and outputs from (b) AMF, (c) FNRM, (d) SSGD C_1 with $a = 0, b = 0.5$ and (e) SSGD C_2 with $a = 0.8, b = 1$.

References

[1] Plataniotis, K.N., and Venetsanopoulos, A.N.: 'Color Image processing and applications' (Springer-Verlag, Berlin, 2000)

[2] Lukac, R., Plataniotis, K.N.: 'A taxonomy of color image filtering and enhancement solutions', in Hawkes, P.W. (Ed.): 'Advances in Imaging and Electron Physics' (Elsevier Acedemic Press, 2006), pp. 187-264

[3] Lucchese, L., and Mitra, S.K.: 'A new class of chromatic filters for color image processing: theory and applications', IEEE Transactions on Image Processing, 2004, 13, pp. 534-548

[4] Morillas, S., Gregori, V., and Sapena, A.: 'Fuzzy Bilateral Filtering for color images', Lecture Notes in Computer Science, 2006, 4141, pp. 138-145

[5] Luszczkiewicz, M., and Smolka, B.: 'Application of bilateral filtering and Gaussian mixture modeling for the retrieval of paintings', Proceedings - International Conference on Image Processing, ICIP, 2009, art. no. 5414097, pp. 77-80

[6] Morillas, S., Gregori, V., and Hervás, A.: 'Fuzzy peer groups for reducing mixed Gaussian-impulse noise from color images', IEEE Transactions on Image Processing, 2009, 18, pp. 1452-1466

[7] Schulte, S., De Witte, V., and Kerre, E.E.: 'A fuzzy noise reduction method for colour images', IEEE Transactions on Image Processing, 2007, 16, pp. 1425-1436

[8] Morillas, S., Schulte, S., Mélange, T., Kerre, E.E., and Gregori, V.: 'A soft-switching approach to improve visual quality of colour image smoothing filters', in: 'Proceedings of Advanced Concepts for Intelligent Vision Systems ACIVS0' (Lecture Notes in Computer Science, 2007,4678), pp. 254-261

[9] Smolka, B. and Plataniotis, K. N.: 'Soft-Switching Adaptive Technique of Impulsive Noise Removal in Color Images', ICIAR, 2005 pp. 686-693

[10] Szczepanski, M., Smolka, B., Plataniotis, K.N., and Venetsanopoulos, A.N.: 'On the distance function approach to color image enhancement', Discrete Applied Mathematics, 2004, 139, pp. 283-305

[11] Elmoataz, A. , Lezoray, O., and Bougleux, S.: 'Nonlocal discrete regularization on weighted graphs: A framework for image and manifold processing', IEEE Transactions on Image Processing, 2008, 17, pp. 1047-1060

[12] De Backer, S., Pizurica, A., Huysmans, B., Philips, W., and Scheunders P.: 'Denoising of multicomponent images using wavelet least-squares estimators', Image and Vision Computing, 2008, 26, pp. 1038-1051

[13] Miller, M., and Kingsbury, N.: 'Image denoising using derotated complex wavelet coefficients', IEEE Transactions on Image Processing, 2008, 17, pp. 1500-1511

[14] Gross, J.L., and Yellen, J.: 'Graph Theory and its applications' (Chapman&Hall CRC, 2nd edn. 2006)

[15] Kerre, E.E.: 'Fuzzy Sets and Approximate Reasoning' (Xian Jiaotong University Press, 1998)

[16] Immerkaer, J.: 'Fast noise variance estimation', Computer Vision and Image Understanding, 1996, 64, pp. 300-302